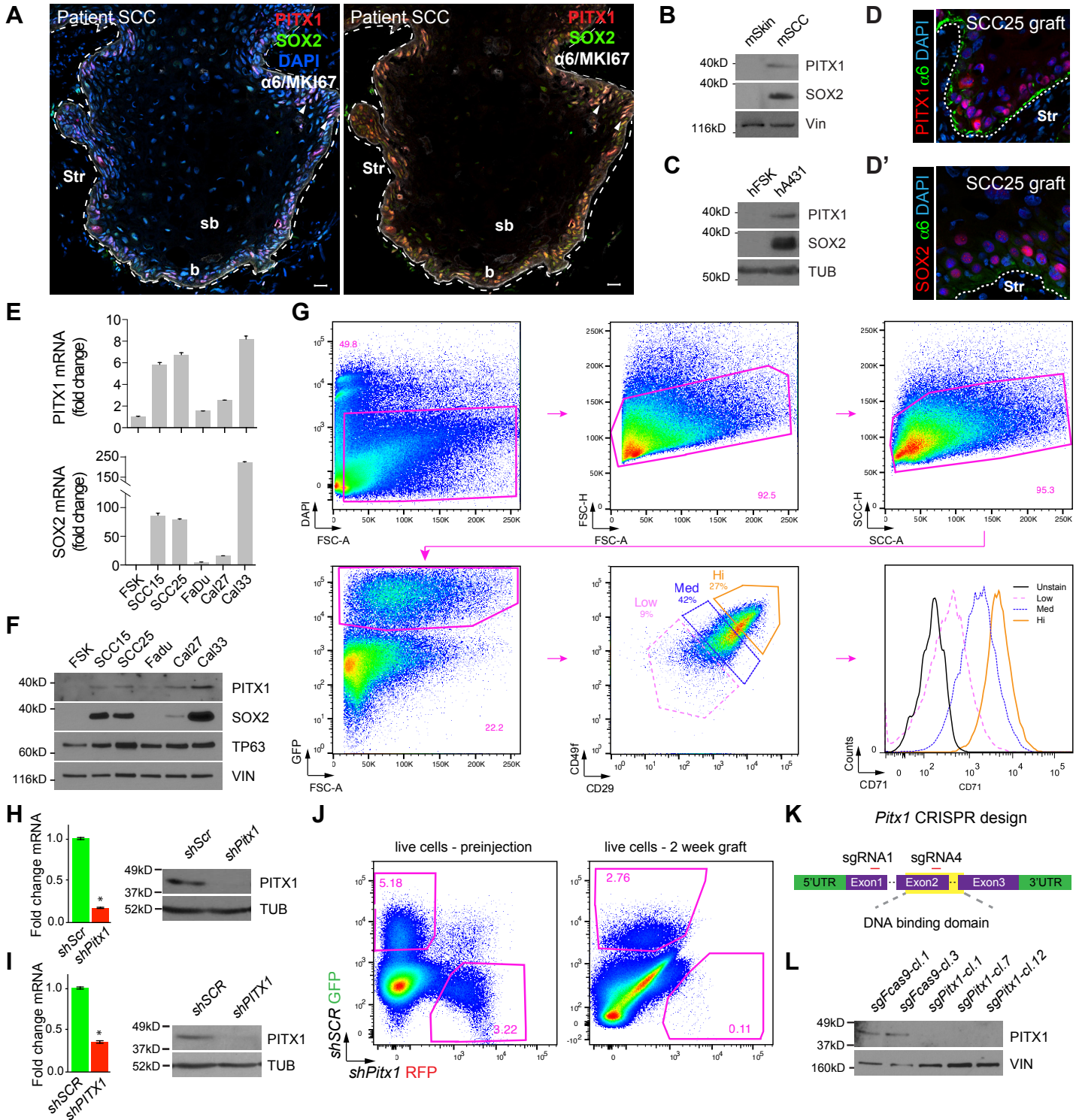

Figure S1, related to Figure 1 and 2. (A) Confocal sections of patient SCC. PITX1 (red) and SOX2 (green) co-localize in basal (b), but not supra-basal (sb) nuclei. White arrows point to MKI67 positive cells (nuclear white). α6 integrin (white line) demarcates the boundary between tumor epithelial and stromal (Str) cells. (B,C) Western blotting detects PITX1 and SOX2 in total protein extracts of (B) DMBA initiated mouse SCC and (C) human A431 culture, but not normal mouse skin or human Foreskin keratinocytes. (D,D') Confocal sections show PITX1 and SOX2 (red) in basal layer of SCC25 (head and neck SCC graft). α6 integrin (green) marks boundary between tumor epithelial and stromal (Str) cells. qPCR (E) and Western blot (F) analyses of PITX1 and SOX2 mRNA and protein expression on a panel of human (HN)-SCC cell lines. Primary human foreskin keratinocyte (FSK) cultures were used as control. (G) Flow cytometric strategy to separate TPCs from differentiated SCC cells in tumor grafts. Live cells are selected based on DAPI exclusion. Next, singlets are selected based on FSC-H/FSC-A and SSC-H/SSC-A ratios before tumor parenchymal cells are isolated based on their H2BGFP lineage marker expression. Finally, the tumor epithelial cell population can be separated into sub-fractions based on their high (Hi), medium (Med) and low α6- and β1-integrin (CD49f and CD29) expression. Transferrin receptor (CD71) expression indicates the cells' proliferative status and allows to reliably separate TPCs from post-mitotic tumor cells. (H, I) qPCRs and Western Blots of Pitx1 expression on mouse (H) or human (I) tumor propagating cells (TPCs) transduced with *shPitx1* or *shScr*. (J) Scatter plots illustrating relative abundance of shScr and shPitx1 transduced tumor epithelial cells at the time of transplantation (pre-injection) and in 2 week SCC grafts. (K) CRISPR design using two gRNAs to delete the DNA binding domain of Pitx1. (L) Analysis of PITX1 protein expression in two control (FCas9), and three *sgPitx1* knock-out clones. Scale bars = 50μm.

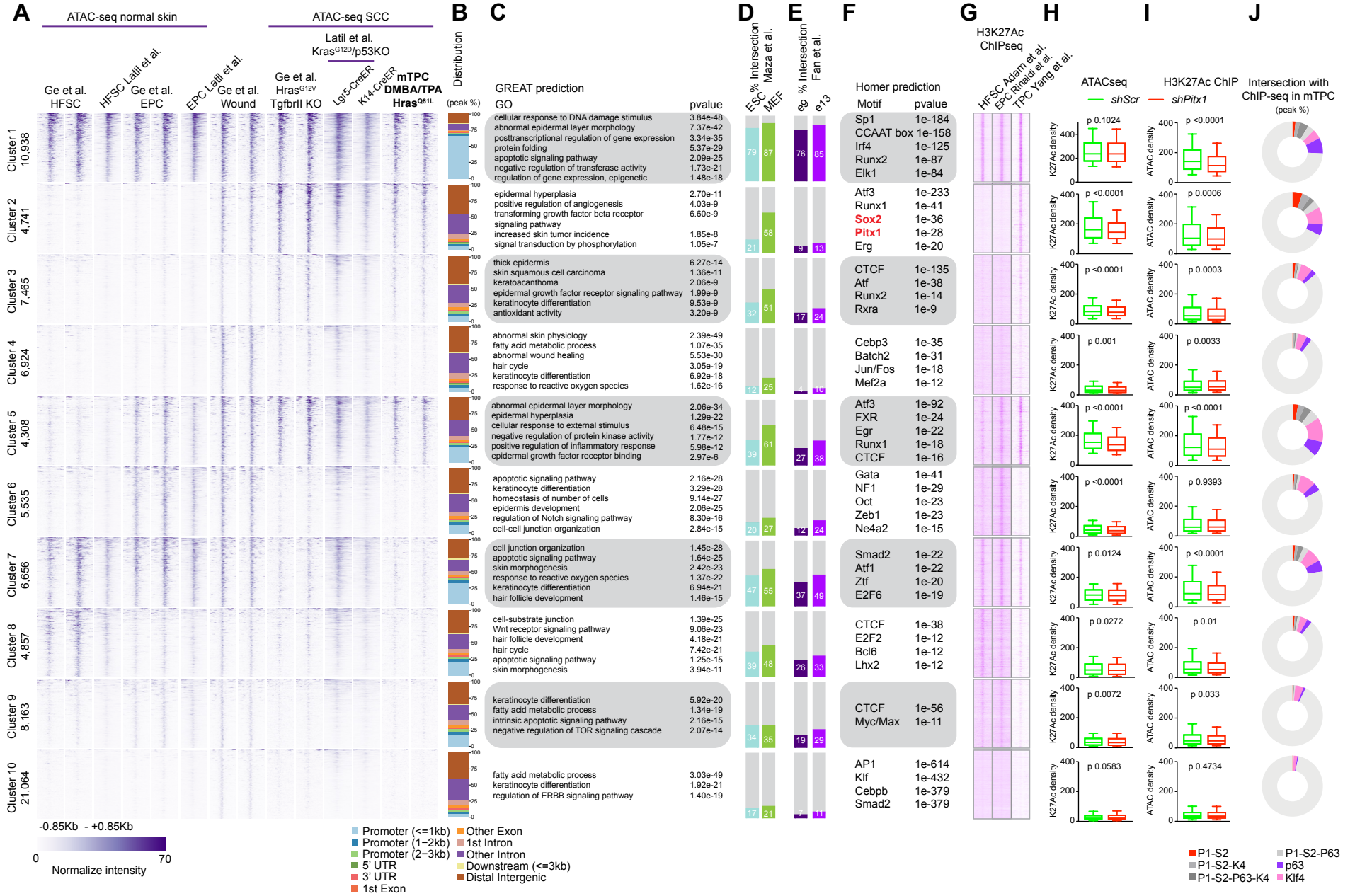

Figure S2, related to Figure 3 and 4. (A) K-Means cluster analyses of different ATAC-seq datasets uncover accessible chromatin in hair follicle stem cells (HFSCs), inter-follicular epidermal progenitor cells (EPCs), wound epithelial cells (wound), and TPCs from three different SCC models (Ge et al. 2017, Latil et al. 2016, and our DMBA induced SCCs). The number of peaks included in each cluster is indicated left side of the cluster. **(B)** Stacked bar graphs represent the relative distribution of ATAC-seq peaks across the genome. Cluster 1 represents constitutively accessible chromatin regions, mostly located at gene promoters. Clusters 2 and 3 contain chromatin that is accessible in SCCs and wound epithelial cells. A majority of these peaks is located at distal intergenic regions and introns. Cluster 7 represents ATAC peaks characteristic of all normal skin epithelial stem and progenitor cell populations. Clusters 6 and 8 depict regulatory elements that characterize EPCs or HFSCs, respectively. **(C)** GREAT analyses predict GO categories significantly enriched in each cluster. **(D-E)** Stacked bar graphs indicate the similarity in chromatin accessibility between TPCs and **(D)** mouse embryonic stem cells (ESC), or embryonic fibroblasts (MEF); or (E) embryonic ectoderm at embryonic day e9 and epidermis at e13. **(F)** HOMER motif predictions discover distinct sets of highly enriched transcription factor (TF) motifs in each cluster. Note: Pitx1 and Sox2 motifs show the highest enrichment in ATAC cluster 2, that is accessible in TPCs. **(G)** Heatmap representing differences in H3K27Ac ChIP-seq densities on TPCs (Yang et al. 2015), EPC (Rinaldi et al. 2017) and HFSC (Adam et al. 2015) in the different ATAC clusters (A). **(H)** Boxplots depict differences in chromatin accessibility between shScr and shPitx1 TPCs isolated directly from SCC grafts. **(I)** Boxplots depict differences in H3K27Ac levels in shScr and shPitx1 transduced TPCs cultures. (H,I) *P<0.0001, Mann-Whitney test, n=2. (J) Donut plots illustrate overlap between ATAC-seq and TF-ChIP-seq peaks shown in Figure 3B. Pitx1 (red, P1), Sox2 (orange, S2), Trp63 (purple, P63) and Klf4 (pink, K4) show highest enrichment in clusters 1,2,5,7.

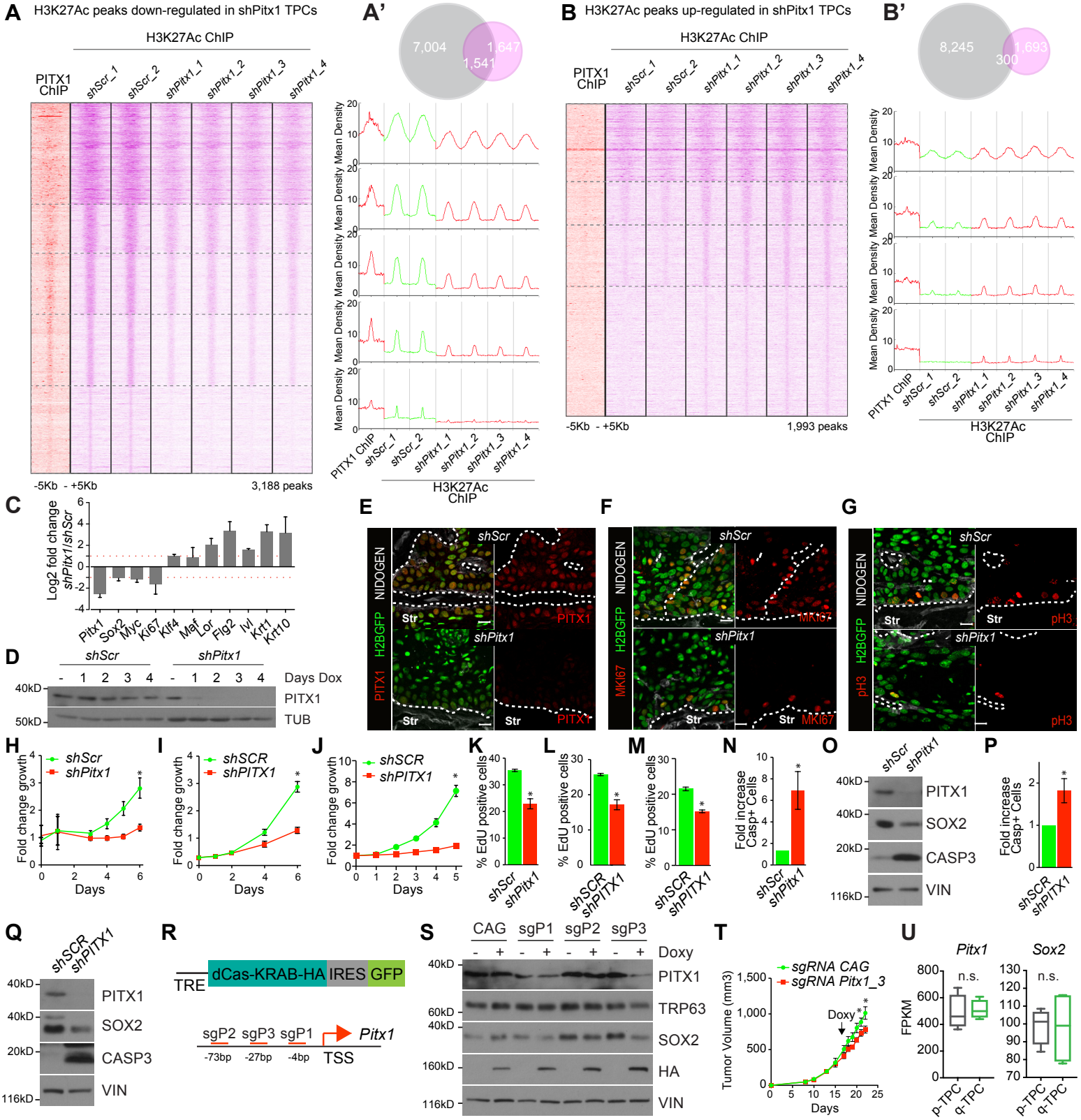

Figure S3, related to Figure 3. (A, B) (left) Heatmap representing differences in H3K27Ac ChIP-seq densities (purple) on *shScr* and *shPitx1* TPCs around K27Ac peaks, which significantly decrease (A) or increase (B) upon *shPitx1* KD. Red histogram shows that Pitx1 ChIP-seq gets enriched on K27Ac peaks that decrease but not in the ones that increase in shPitx1 TPCs. Dotted lines indicate clusters based on K27Ac signal intensity differences. (Right) Mean density of Pitx1 and H3K27Ac ChIP-seq on the different clusters. (A' and B') Intersection of Pitx1 bound peaks in Pitx1 ChIP-seq with H3K27Ac peaks that get significantly down- (A') or up regulated (B') in shPitx1 TPCs.(C) qRT-PCR data confirming changes in epidermal differentiation marker expression upon in *shPitx1* in TPCs isolated from four independent SCCs (mean±s.e.m, n=4; *P<0.05, Student's t-test). (D) Western blotting confirming PITX1 depletion in TPC cultures transduced with a Dox inducible *shPitx1* (E-G). Representative confocal images of TPC grafts expressing Dox inducible *shScr* or *shPitx1* after 10 days on Dox. Images show decreased PITX1 (E), MKI67 (F) or pH3 (G) expression (red) in *shPitx1* tumors. H2BGFP marks the tumor parenchyma. NIDOGEN (white) demarcates the basement membrane. Scale bars=50μm. (H-J) Growth analyses of *shScr* and *shPitx1* infected murine TPCs (H), A431 human SCCs (I) and Cal33 human (HN)-SCCs (J) (mean±s.e.m., n=3, *P<0.05, Student's t-test). (K-M) EdU incorporation analyses show decreased proliferation in *shPitx1*-infected murine TPCs (K), A431 SCCs (L) and Cal33 HN-SCCs (M) (mean±s.e.m., n=3, *P<0.05, Student's t-test). (N,P) Flow cytometric analyses of active Caspase-3 reveal increased apoptosis rates in *shPitx1*-transduced murine TPCs (N) and human A431 SCCs (P). (O,Q) Western blot analyses of PITX1, SOX2 and active Caspase-3 in *shScr* and *shPitx1* transduced mouse TPCs (O) and Cal33 HN-SCCs (Q). (R) Inducible CRISPR interference construct and sgRNAs targeting *Pitx1* promoter (sgP1-3). sgRNAs are located at different distance from the TSS. (S) Western-blotting of primary TPCs infected with inducible CRISPRi construct and 3 different sgRNAs targeting the PITX1 promoter (sgP1-3) or a control (sgCAG) treated for two days with Doxycycline (Dox), showing decreased PITX1, SOX2 and TRP63 protein levels on the sgP_3. HA indicates the induction of dCas9-KRAB. (T) Line graphs indicate significantly reduced growth rate of Dox-inducible CRISPRi sgPitx1_3, compared to sgCAG controls in fully established murine SCCs (mean±s.e.m, n=6, *P<0.05, Sidak's multiple comparisons test). (U) Boxplots depict no significant differences in Pitx1 (left) or Sox2 (right) expression levels between proliferative (pTPC) and quiescent TPCs (qTPCs) identified by H2BGFP pulse-chasing and label retention.

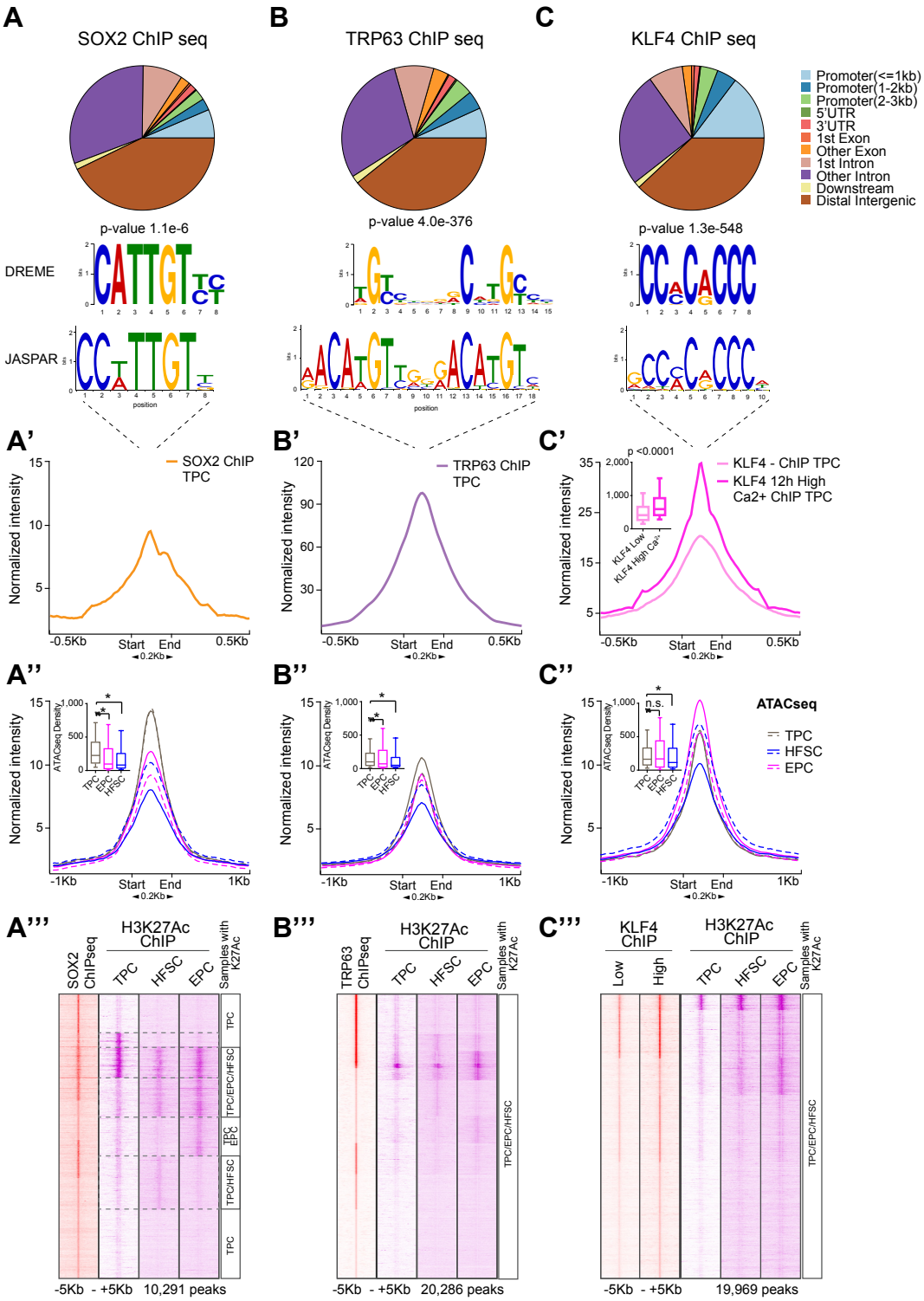

Figure S4, related to Figure 4. (A, B, C) Pie charts illustrate the relative distribution of SOX2 (A), TRP63 (B) and KLF4 (C) bound regulatory sequences across the genome. These transcription factors are mostly enriched on intronic and distal intergenic chromatin. SOX2 (A'), TRP63 (B') and KLF4 (C') motifs are discovered de novo with MEME and CentriMo at peak centers. Histograms represent normalized SOX2 (orange), TRP63 (purple) and KLF4 (pink) ChIP-seq intensities in TPC. Mean ATACseq (A''-C'') signal intensity in TPCs (grey), HFSCs (blue), and EPCs (pink) surrounding SOX2 (A''), TRP63 (B'') and KLF4 (C'') bound loci. (C'') Boxplots depict KLF4 ChIP-seq signal in Low and High Calcium around KLF4 bound regions (*P<0.0001, Mann-Whitney test). (A'''-C''') Heatmap representing SOX2 (A'''), TRP63 (B''') and KLF4 (C''') ChIP-seq (red) read densities centered around their peak summits on chromatin from primary TPC cultures. Purple tracks show the H3K27Ac ChIP-seq densities on TPCs, EPC and HFSC.

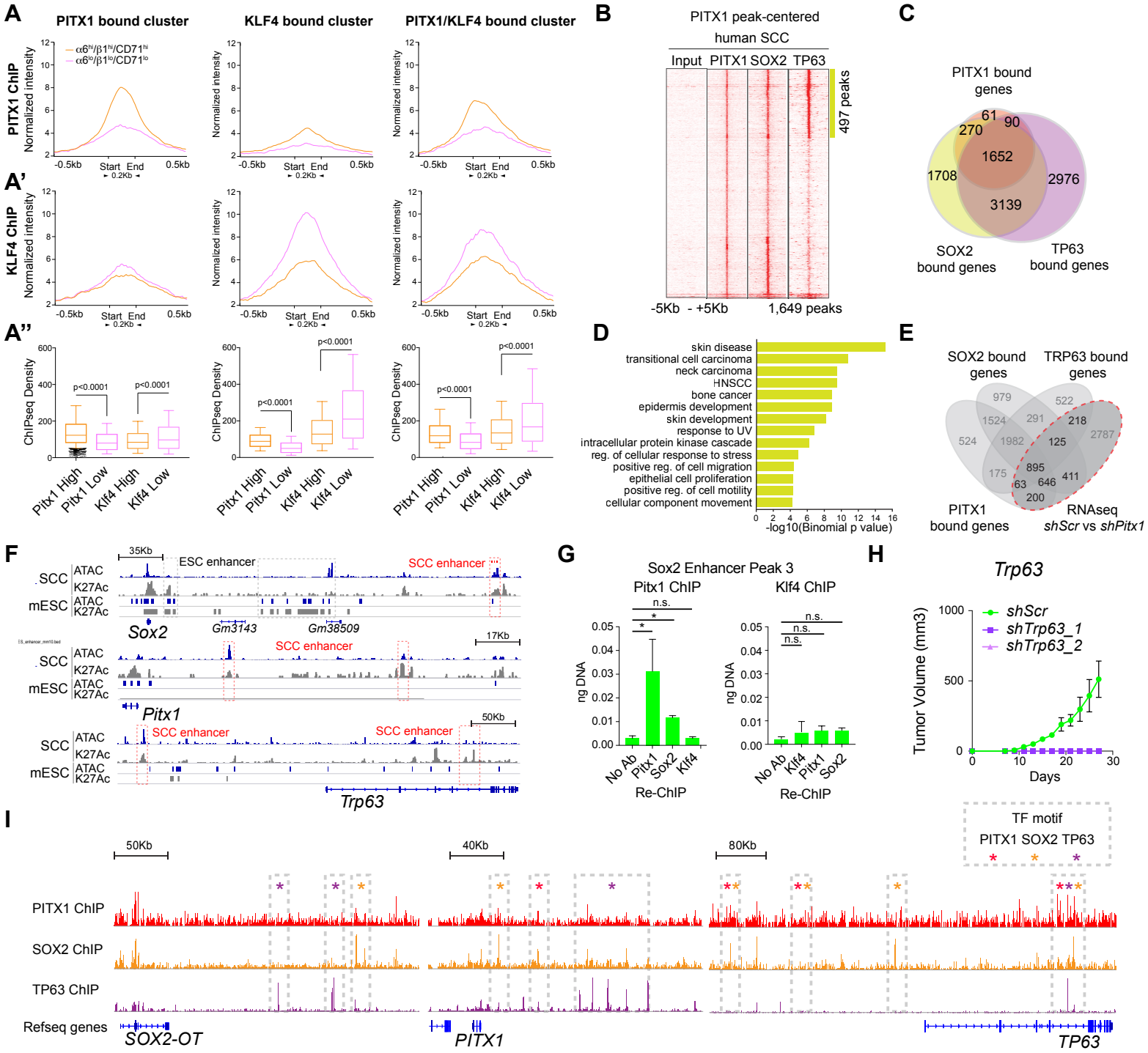

Figure S5, related to Figures 4 and 5. (A) Histograms represent mean PITX1 and KLF4 ChIP-seq signal on α6^{hi}β1^{hi}CD71^{hi} (orange) and α6^{lo}β1^{lo}CD71^{lo} SCC cells at PITX1 (clusters 1&4, Figure 4D), KLF4 (cluster 6, Figure 4D) and PITX1/KLF4 (clusters 2&3, Figure 4D) bound clusters. Boxplots depict normalized PITX1 and KLF4 ChIP-seq intensity in α6^{hi}β1^{hi}CD71^{hi} and α6^{lo}β1^{lo}CD71^{lo} SCC cells (P<0.0001, Mann-Whitney test. n=1). (B) Heatmaps of PITX1-centered, K-means clustered ChIP-seq peaks of human SCC25 cells. (C) Venn diagram shows genes associated with SOX2, PITX1 and TP63 peaks. (D) GREAT analysis show GO terms of genes associated with PITX1, SOX2, and TP63 on the indicated cluster. (E) Venn diagram shows intersection of genes, which are PITX1, SOX2 and TRP63 bound and increased or decreased in expression upon *Pitx1* knock-down. (F) ATAC-seq (blue) and H3K27 acetylation ChIP-seq (grey) tracks (SCC) or boxes (ESC) reveal novel SCC specific enhancers (red dotted boxes). Note that the *Sox2* enhancer of ESCs (grey dotted boxes) is different from the TPC enhancer. *Pitx1* and *Trp63* associated TPC enhancers are inactive in ESC and ESC enhancers are inactive in TPCs. (G) Bar graphs depict enrichment of Sox2 enhancer peak 3 sequence (Figure 5A) after PITX1 or KLF4 ChIP and re-ChIP with anti-PITX1, anti-SOX2 and anti-KLF4 antibodies indicating physical interactions between SOX2 and PITX1 but not KLF4 at this gene regulatory element. (H) Line graphs depict tumor volume of control (green) and *Trp63* depleted (pink and purple) mouse SCCs over time (days). Graph shows mean ±s.e.m. (n=6, *P<0.05). (I) PITX1 (red), SOX2 (orange) and TP63 (purple) ChIP-seq tracks indicate enrichment of these transcription factors at the *SOX2*, *PITX1* and *TP63* genomic loci. Dotted boxes highlight putative enhancers. Asterisks mark PITX1 (red), SOX2 (orange) of TP63 (purple) transcription factor motifs. **See also Table S3 and 5.**

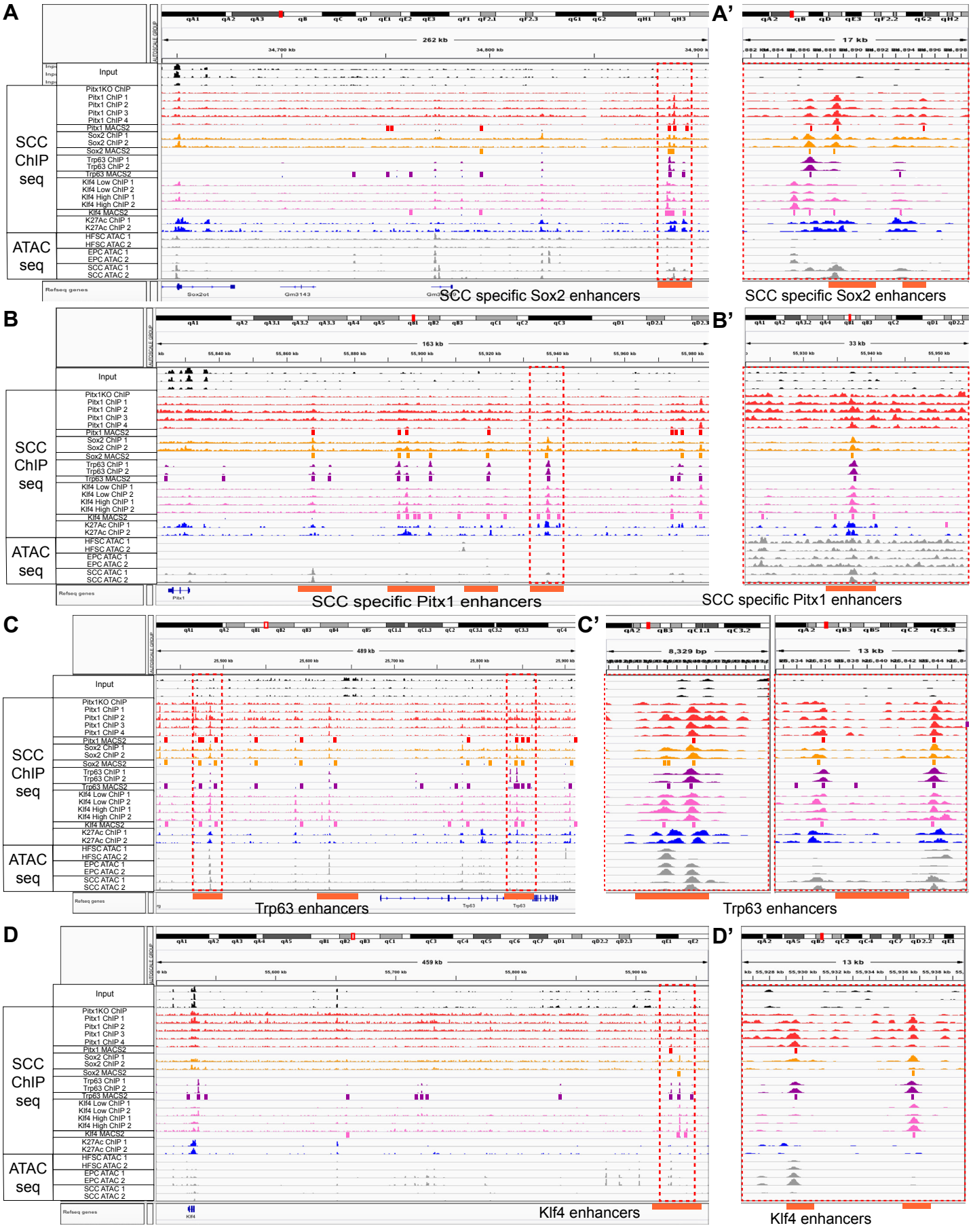

Figure S6, related to Figure 5 and 6. Genome browser screen-shot of our ChIP-seq and ATAC-seq tracks along with MACS2 peak calling at the SCC specific Sox2 (A,A'), Pitx1 (B,B'), Trp63 (C,C') and Klf4 (D,D') enhancer.

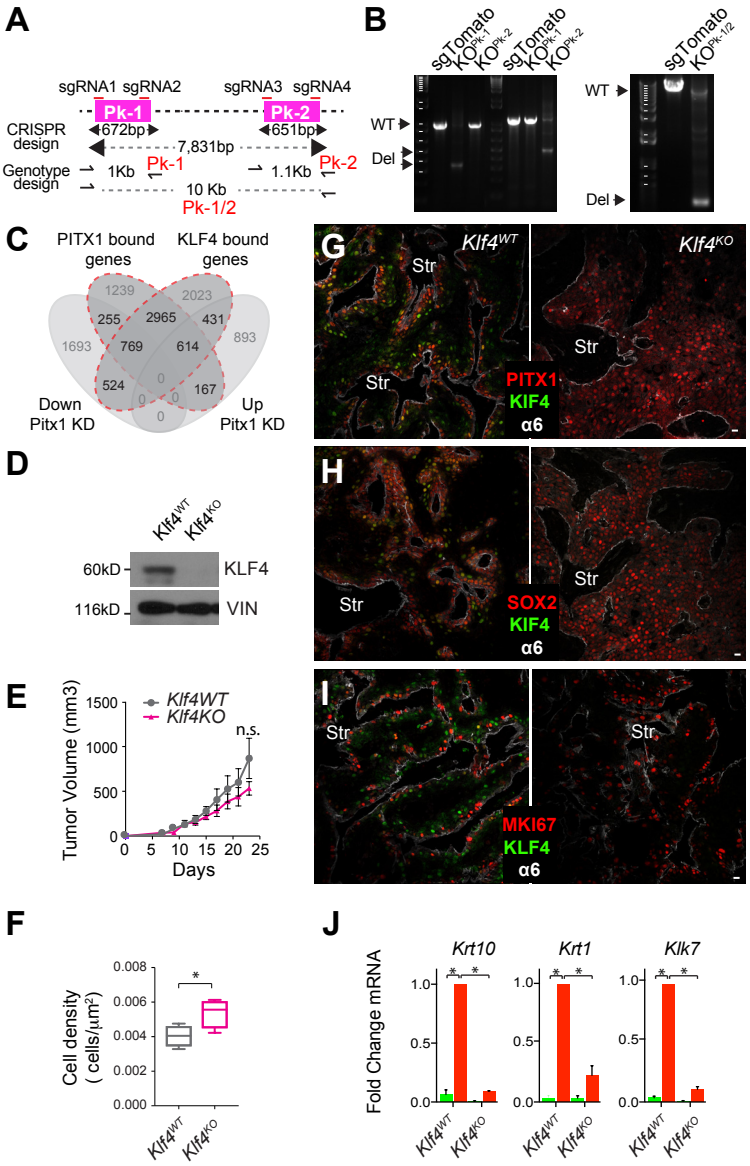

Figure S7, related to Figure 6 and 7. (A) CRISPR strategy to delete the KLF4 enhancer peak-1 (Pk-1), Pk-2, or Pk-1+2 with two gRNAs pairs. (B) Genotyping confirms the KLF4 enhancer deletions described in (A). (C) Venn diagram depicting PITX1 and KLF4 bound genes as well as up and down-regulated transcripts after Pitx1 knock-down. (D) Western blots indicate effective Klf4 knock-out. (E) Line graphs depict tumor volume of Klf4WT (grey) and Klf4KO (purple) SCCs over time (days). Data are presented as mean, with error bars indicating ±s.e.m. (n=3, *P<0.05, Student's t-test). (F) Box-Plots illustrate cell density in murine Klf4WT and Klf4KO (n=4, *P<0.05, Student's t-test) SCCs. (G-I) Confocal images of Klf4KO SCC show aberrant supra-basal (SB) PITX1 (G) SOX2 (H) and MKI67 (I) expression. Scale bars, 50µm. (J) qRT-PCR shows fold change differences of select KLF4 and PITX1 target genes in Klf4WT and Klf4KO TPCs after shScr or shPitx1 knock-down. Data are represented as mean with error bars indicating ±s.e.m. (n=2, *P<0.05, Student's t-test). **See also Table S6.**